

Thermal and optical gaps in nearly-one-dimensional compounds

G. Mihály and A. Virosztek

*Institute of Physics, Technical University of Budapest, H-1111 Budapest, Hungary
and Research Institute for Solid State Physics, P.O. Box 49, H-1525 Budapest, Hungary*

G. Grüner

Department of Physics, University of California at Los Angeles, Los Angeles, California 90024

(Received 22 January 1997)

We discuss the consequences of the dispersion of the energy bands in the broken symmetry (charge- and spin-density-wave) states of highly anisotropic metals. Such dispersion becomes important with increasing deviations from perfect nesting, and leads to differences between the gaps as sampled by transport and optical measurements. We discuss the available experimental results obtained in a variety of materials with different band-structure anisotropy. [S0163-1829(97)50324-9]

I. INTRODUCTION

In strictly one dimension the $2k_F$ singularity of the Lindhardt response function leads to broken symmetry, charge- and spin-density-wave ground states.¹ These states, predicted by theory decades ago, have by now been found in a variety of so-called linear chain compounds, where the weak transfer integral perpendicular to the chains, which we call t_b and t_c throughout this paper, together with a sizable transfer integral t_a in the chain direction, lead to a highly anisotropic band structure.

The deviation from strict one dimensionality in the materials which can be synthesized has several important consequences. First, there is a large fluctuation region below the temperature T_{MF} , the temperature where the mean-field solution leads to a phase transition. Second, there is a phase transition at $T_{3D} < T_{MF}$ where long-range order develops. The fundamental consequence of the above is (among others) the fact that the single-particle gap measured well below the transition T_{3D} is significantly larger than that predicted by the weak-coupling BCS limit, $2\Delta = 3.5kT_{3D}$, even in cases where the coupling is weak. The reason for this is that the single-particle gap is related to T_{MF} , while the transition temperature is determined, among other factors by the (weak) interchain interactions. This aspect of low-dimensional metals is by now fully explored and understood.¹

In this paper we discuss another consequence of the deviations from the one-dimensional limit, which naturally gives rise to perfect nesting with the nesting wave vector k_F lying along the direction a . With b and c directions included, the Fermi surface consists of two parallel sheets, and the gap does not have a dispersion. In the case of (weak) two- or three-dimensional band structure, when the nesting is still fully satisfied, the nesting wave vector includes both in-chain, k_x and perpendicular to the chain, k_y and k_z components.²⁻⁴ When such a nesting condition is not fulfilled (the situation we discuss later), the energy levels near to the gap have a dispersion which can be calculated using straightforward band theory with simple assumptions. This, in turn, leads to differences between the direct gap (as mea-

sured by optics) and the indirect gap (as sampled by the temperature-dependent dc conductivity well below the gap). We review the available experimental results which confirm the above picture. We also discuss cases where a semimetallic state is recovered and suggest examples of such cases.

II. THEORY

While several authors have considered the case of anisotropic band structure, and nonperfect nesting,²⁻⁶ we recall the main results, before giving expressions for the various single-particle gaps. We use a highly anisotropic nearest neighbor tight-binding model³

$$\varepsilon(\mathbf{k}) = -2t_a \cos(ak_x) - 2t_b \cos(bk_y) - 2t_c \cos(ck_z) - \mu, \quad (1)$$

where μ is the chemical potential, a , b , and c are the orthorhombic lattice constants, and $t_a \gg t_b \gg t_c$ are the hopping integrals in the three directions. A linearized dispersion with the same Fermi surface is given by⁴

$$\tilde{\varepsilon}(\mathbf{k}) = v_F(|k_x| - \bar{k}_F) - 2t_b \cos(bk_y) - 2t'_b \cos(2bk_y) - 2t_c \cos(ck_z), \quad (2)$$

with $v_F = 2at_a \sin(ak_F)$, $a\bar{k}_F = ak_F - t_b^2 \cos(ak_F) / 4t_a^2 \sin^3(ak_F)$, and

$$t'_b = -\frac{t_b^2 \cos(ak_F)}{4t_a \sin^2(ak_F)}. \quad (3)$$

Note that the band filling is now determined by \bar{k}_F , although it differs from k_F only by a few percent.

It is easy to see that for a spectrum given by Eq. (2), the best nesting vector is

$$\mathbf{Q} = (2\bar{k}_F, \pi/b, \pi/c), \quad (4)$$

i.e., the Linhard function has its maximum at this wave vector. In the density-wave state the order parameter $|\Delta|$ couples

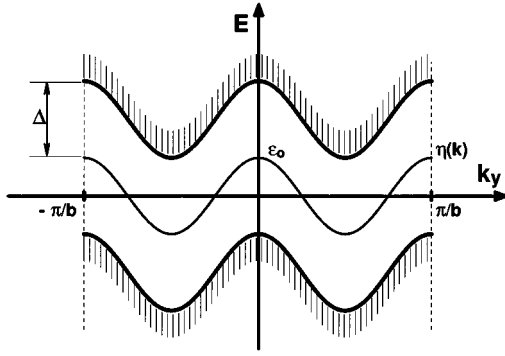


FIG. 1. The upper and lower edges of the density wave gap are shown as a function of k_y , the wave number perpendicular to the chains. $\eta(\mathbf{k})$ is defined by Eq. (7).

the states \mathbf{k} and $\mathbf{k}-\mathbf{Q}$, and opens a gap at the Fermi energy around $k_x \approx \tilde{k}_F$. The new spectrum consists of two bands given by⁵

$$E_{\pm}(\mathbf{k}) = \eta(\mathbf{k}) \pm \sqrt{|\Delta|^2 + [\xi(\mathbf{k})]^2}, \quad (5)$$

where $\eta(\mathbf{k}) = [\varepsilon(\mathbf{k}) + \varepsilon(\mathbf{k}-\mathbf{Q})]/2$ and $\xi(\mathbf{k}) = [\varepsilon(\mathbf{k}) - \varepsilon(\mathbf{k}-\mathbf{Q})]/2$. In terms of the equivalent dispersion [see Eq. (2)],

$$\xi(\mathbf{k}) = v_F(k_x - \tilde{k}_F) - 2t_b \cos(bk_y) - 2t_c \cos(ck_z) \quad (6)$$

and

$$\eta(\mathbf{k}) = -2t'_b \cos(2bk_y) = \varepsilon_0 \cos(2bk_y), \quad (7)$$

where we introduced the ‘‘unnesting’’ parameter

$$\varepsilon_0 = \frac{t_b^2 \cos(ak_F)}{2t_a \sin^2(ak_F)} \quad (8)$$

instead of t'_b . The thermodynamics of this model has been studied quite extensively.⁶

Here we focus on the optical and the thermal gap in the density wave state. The optical gap is the minimum energy required for a $\mathbf{q}=0$ excitation, i.e., for the spectrum given by Eq. (5):

$$G^{\text{opt}} = \text{Min}\{2\sqrt{|\Delta|^2 + [\xi(\mathbf{k})]^2}\} = 2|\Delta|. \quad (9)$$

The thermal gap is the difference between the lower edge of the upper band and the upper edge of the lower band. Compared to the optical gap, momentum conservation is relaxed here, therefore $G^{\text{th}} \leq G^{\text{opt}}$. As in the previous case,

minimizing the square root in E_{\pm} with respect to k_x yields $|\Delta|$ (note that η does not depend on k_x), therefore the thermal gap is

$$G^{\text{th}} = 2|\Delta| - 2|\varepsilon_0| = 2|\Delta| - \frac{t_b^2 |\cos(ak_F)|}{t_a \sin^2(ak_F)}. \quad (10)$$

The gap structure is shown in Fig. 1.

The quantity which we will discuss is the ratio of the two gaps,

$$\frac{G^{\text{th}}}{G^{\text{opt}}} = 1 - \frac{|\varepsilon_0|}{|\Delta|} = 1 - \frac{|\cos(ak_F)|}{\sin^2(ak_F)} \frac{t_b^2}{t_a G^{\text{opt}}} \equiv 1 - x. \quad (11)$$

For a half filled band, $G^{\text{th}} = G^{\text{opt}}$, and, for a quarter-filled band,

$$\frac{G^{\text{th}}}{G^{\text{opt}}} = 1 - \sqrt{2} \frac{t_b^2}{t_a G^{\text{opt}}} \equiv 1 - x_{\text{quarter}}. \quad (12)$$

III. ANALYSIS OF EXPERIMENTS

Next we discuss the experimental results obtained in several highly anisotropic metals with charge-density-wave (CDW) and spin-density-wave ground states. The band-structure parameters t_a , t_b , and t_c have been deduced from measurements such as magnetic susceptibility, specific heat, and dc transport anisotropy. The thermal and optical gaps have been measured in several highly anisotropic metals with charge- and spin-density-wave ground states. The transport gaps are inferred from the exponential temperature dependence of the dc conductivity at temperature ranges well below the transition temperature. The optical gaps are determined from optical experiments with an appropriate analysis which takes into account the one-dimensional (1D) density of states and also some fluctuation effects in the CDW states. The relevant data are collected in Table I. In most cases the band filling is $\frac{1}{4}$ or $\frac{3}{4}$ [giving also Eq. (12)], although in some cases an observed dimerization may lead to some complications. There are also differences in the relevant dimensionality. For KCP the two perpendicular transfer integrals are the same, both significantly smaller than t_a . This situation is somewhat different than the model we examined, but can (for the particular crystal structure of the compound) be reduced to an effective 2D model with an effective t_a larger by a factor of 2 than $t_b = t_c$ as given by the band-structure calculations. For the other compounds the two perpendicular transfer integrals are different, one significantly larger than

TABLE I. The experimental values of the thermal gap, optical gap, band filling, overlap integral, and conduction anisotropy for various low-dimensional metals.

	G^{th} (K)	G^{opt} (K)	Filling	t_a (K)	σ_b/σ_a	x
(TaSe ₄)I ₂	3000 (Refs.1,7)	2900 (Ref. 1)	1/4	12 000 (Ref. 9)	$\approx 10^4$ (Ref. 9)	≈ 0
KCP	1400 (Ref. 10)	1700 (Ref. 1)	5/6 (Ref. 11)	10^4 (Ref. 8)	10^4 (Ref. 12)	≈ 0
TaS ₃	1600 (Ref. 1)	1800 (Ref. 1)	1/4	2280 (Ref. 1)	300 (Ref. 13)	0.005
K _{0.3} MoO ₃	920 (Ref. 1)	1400 (Ref. 1)	3/4	9300 (Ref. 14)	30 (Ref. 15)	0.34
(TMTSF) ₂ PF ₆	46 (Ref. 16)	101 (Ref. 17)	3/4	3000 (Ref. 16)	100 (Ref. 16)	0.42
(TMTSF) ₂ PF ₆ -6 kbar	26 (Ref. 18)	101	3/4	5600 (Ref. 18)	100	0.84
NbSe ₃	-30 (Ref. 21)	230 (Ref. 19)	1/4	3300 (Ref. 20)	25 (Ref. 20)	-0.13

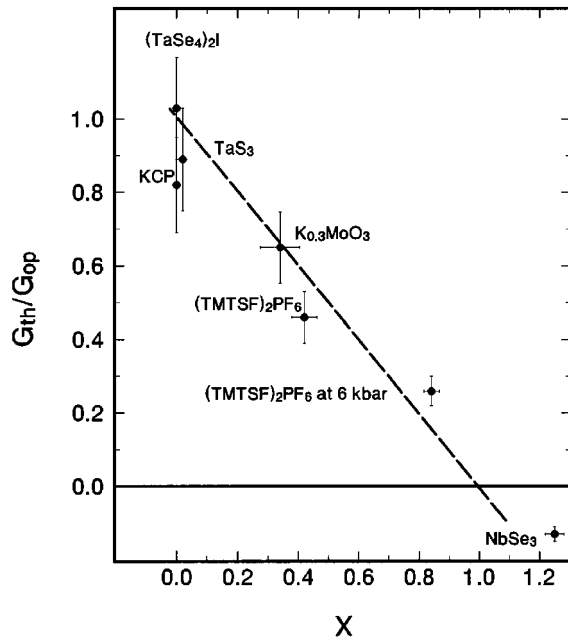


FIG. 2. The ratio of the thermal and optical gaps as functions of the anisotropy parameter defined in Eqs. (11) and (12). The dashed line is Eq. (11) with the parameter x calculated for each compound using data given in Table I. The error bars correspond to 10% uncertainty both in the transport and optical data.

the other. For these compounds the smaller transfer integral (which leads to 3D character) is neglected, and we use a 2D model in accordance of the calculations detailed above. Consequently in all cases we use Eq. (11) to compare the optical and transport gaps.⁷⁻²⁰

In Fig. 2, we display the ratio of the two gaps as function of x , defined in Eq. (11). Materials with a highly anisotropic band structure, such as KCP and $(\text{TaSe}_4)_2\text{I}$ have, within experimental error, the same optical and transport gaps, and the difference increases with increasing 2D character, in full agreement with theory, given by the dashed line in Fig. 2

The model also predicts a transition from a semiconducting to semimetallic state, when the lower and upper bands overlap and G^{th} is negative. This occurs when

$$2|\Delta| = \frac{t_b^2 |\cos(ak_F)|}{t_a \sin^2(ak_F)}. \quad (13)$$

We believe there are several examples of a scenario where, due to increased t_b/t_a the ground state is a semimetal. The linear chain compound NbSe_3 remains highly conducting below its CDW transitions with an optical gap estab-

lished in the broken symmetry, but conducting state. Tunneling experiments on this compound were interpreted recently using the same model we discussed above, and the parameters pertaining to our discussion have been evaluated.²¹ We note, however, that this simple model cannot be extended above $x=1$, where the unnesting drives the density-wave transition temperature to zero.⁶

IV. CONCLUSIONS

In conclusion, we have presented a simple picture which explains the observed differences between the transport and optical gaps measured in several linear chain compounds. In the model, deviations from one dimensionality are intimately related to such differences, and should be a general feature of anisotropic materials. Experiments in other materials, such as $(\text{TMTSF})_2\text{ClO}_4$, where the perpendicular transfer integrals are larger than in the semiconducting compounds we discussed, would be desirable. Low-temperature extension of the high resolution angle resolved photoemission studies performed in linear chain compounds²² may directly test the band dispersion discussed above. It is also conceivable that the overall picture has a more general validity, and can explain the features of materials with various ground states and metallic behavior. In the spin-density-wave state of Cr and also in several heavy fermion compounds such as URu_2Si_2 and UCu_5 , dc transport measurements give evidence for the partial removal of the Fermi surface at the magnetic phase transition, and optical experiments establish a single-particle gap.²³ We suggest that in these materials a similar picture may be appropriate.

Finally we note that the picture we have discussed completely neglects the effects of electron-electron interactions — except of course those which lead to phase transitions. The transition from semiconductor to semimetal as the function of the parameter x is consequently a genuine band-crossing transition. Interaction effects may lead to low-lying states close to the transition at $x=1$ which are fundamentally different from the single-particle states suggested by band theory. Various theories, which address the question of phase transitions in coupled interacting chain systems, may give an answer to the above question.

ACKNOWLEDGMENTS

This work was supported by the U.S.–Hungarian Science and Technology Joint Fund under Project No. 264, and by the Hungarian National Research Fund under Grant Nos. OTKA T07277, T15552, and T020030 and by NSF Grant No. INT-9322517.

¹G. Gruner, *Density Waves in Solids* (Addison-Wesley, New York, 1994).

²B. Horowitz, H. Gutfreund, and M. Weger, *Phys. Rev. B* **12**, 3174 (1975); S. Jafarey, *ibid.* **16**, 2584 (1977); X. Huang and K. Maki, *ibid.* **40**, 2575 (1989).

³K. Yamaji, *J. Phys. Soc. Jpn.* **51**, 2787 (1982).

⁴L. P. Gorkov and A. G. Lebed, *J. Phys. (France) Lett.* **45**, 433 (1984).

⁵See, e.g., K. Maki and A. Virosztek, *Phys. Rev. B* **41**, 557 (1990), and references therein.

- ⁶Y. Hasegawa and H. Fukuyama, *J. Phys. Soc. Jpn.* **55**, 3978 (1986); X. Huang and K. Maki, *Phys. Rev. B* **42**, 6498 (1990); **46**, 162 (1992).
- ⁷Z. Z. Wang *et al.*, *Solid State Commun.* **46**, 325 (1983).
- ⁸K. Carneiro, in *Electronic Properties of Inorganic Quasi-One-Dimensional Materials*, edited by P. Monceau (Reidel, Dordrecht, 1985), Part II, p. 3.
- ⁹H. P. Geserich, in *Electronic Properties of Inorganic Quasi-One-Dimensional Materials* (Ref. 8), p. 111.
- ¹⁰H. Nagosawa, *J. Phys. Soc. Jpn.* **45**, 701 (1978).
- ¹¹R. Comes, M. Lambert, H. Launois, and H. R. Zeller, *Phys. Rev. B* **8**, 571 (1973).
- ¹²J. Bernasconi, P. Bruschi, and H. R. Zeller, *J. Phys. Chem. Solids* **35**, 145 (1974); H. R. Zeller and A. Beck, *ibid.* **35**, 77 (1974).
- ¹³Zhang Dian-lin, Wu Pei-jun, Chen Xin-fen, Duan Hong-min, and Lin Shu-yuan, *Solid State Commun.* **61**, 377 (1987).
- ¹⁴D. C. Johnston, *Phys. Rev. Lett.* **52**, 2049 (1984).
- ¹⁵C. Schlenker and J. Dumas, in *Crystal Chemistry and Properties of Materials with One-Dimensional Structures*, edited by J. Rouxel (Reidel, Dordrecht, 1986).
- ¹⁶D. Jerome and H. J. Schulz, *Adv. Phys.* **31**, 299 (1982).
- ¹⁷L. Degiorgi *et al.*, *Phys. Rev. Lett.* **76**, 3838 (1996).
- ¹⁸N. Biskup, S. Tomic, and D. Jerome, *Phys. Rev. B* **51**, 17 972 (1995).
- ¹⁹W. A. Challander and P. L. Richards, *Solid State Commun.* **52**, 117 (1984).
- ²⁰J. A. Wilson, *Phys. Rev. B* **19**, 6456 (1979).
- ²¹J. P. Sorbier, H. Tortel, P. Monceau, and F. Levy, *Phys. Rev. Lett.* **76**, 676 (1996).
- ²²M. Grioni, H. Berger, M. Garnier, F. Bommeli, L. Degiorgi, and C. Schlenker, *Phys. Scr.* **T66**, 172 (1996), and references therein.
- ²³See, e.g., *Proceedings of the International Conference on Strongly Correlated Electron Systems, Zurich 1996* [*Physica B* (to be published)].